Attowatt Sensitivity of the Capacitively-Coupled Cold Electron Bolometer

Ian Jasper A. Agulo, Leonid S.Kuzmin, and Michael A. Tarasov

***Abstract*—We have fabricated and characterized the Cold-Electron Bolometer (CEB) in the current-biased mode. We measured the bolometer responsivity and the noise equivalent power (NEP) by applying a modulated heating current through the absorber. The frequency of modulation varied from 35 Hz to 2 kHz. The best responsivity of 1.5×10^{10} V/W was obtained at 35 Hz. NEP of better than 10^{-18} W/Hz$^{1/2}$ was measured for modulation frequencies above than 100 Hz. The background power load and the bolometer time constant was also estimated using the experimental device parameters.**

***Index Terms*—Cold-Electron bolometer, Noise Equivalent Power, Responsivity, SIN tunnel junction**

I. Introduction

The highest level of requirements for detectors in the near future will be determined by the proposed NASA missions SPIRIT, SPECS and SAFIR. The detector goal is to provide noise equivalent power down to 10^{-20} W/Hz$^{1/2}$ [1] over the 40 – 500 μm wavelength range in a 100x100 pixel detector array with low power dissipation array readout electronics. To the author's knowledge, the transition-edge sensor (TES) with a strong electrothermal feedback [2,3] is the current detector technology of choice. However, the limitations in its sensitivity are excess noise, saturation and overheating from the dc power for the feedback. To achieve high sensitivity, the concept of the Cold-Electron Bolometer (CEB) with strong electrothermal feedback [4] has been proposed.

Manuscript received May 31, 2005. This work was supported by The Swedish Research Council (Vetenskapsrådet), The Swedish Foundation for International Cooperation in Research and Higher Education (STINT), and the Swedish Institute (SI).

I. J. A. Agulo is with the Quantum Device Physics Laboratory, Department of Microtechnology and Nanoscience, Chalmers University of Technology SE-41296 Gothenburg, Sweden, on leave from the Department of Physics, University of the Philippines Baguio, Gov. Pack Road, 2600 Baguio City, Philippines (e-mail: ian.agulo@ mc2.chalmers.se).

L. S. Kuzmin is with the Quantum Device Physics Laboratory, Department of Microtechnology and Nanoscience, Chalmers University of Technology SE-41296 Gothenburg, Sweden, and is also affiliated to Moscow University, Nuclear Physics Institute, 119899 Moscow, Russia (corresponding author: +46(31)-772-3608; fax: +46(31)-772-3471; e-mail: leonid.kuzmin@mc2.chalmers.se).

M. A. Tarasov is with the Quantum Device Physics Laboratory, Department of Microtechnology and Nanoscience, Chalmers University of Technology SE-41296 Gothenburg, Sweden (e-mail: mikhail.tarasov@mc2.chalmers.se).

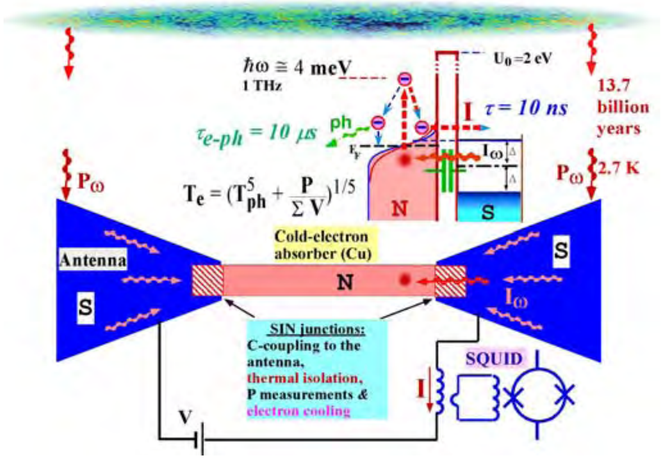

Fig. 1. Principle of the CEB. Radiation from space is detected by the antenna, which then focuses the incoming signal to the absorber. The electromagnetic signal goes through the superconductor-insulator-normal metal (SIN) tunnel junctions, and its energy is transferred to the normal metal electrons. The relaxation of electron energy occurs in two ways. The first is relaxation by electron-phonon interaction, and the second is extraction of hot electrons from the normal metal by the cooling current of the SIN tunnel junction. The fastest process determines the bolometer response. The ideal case would then be the electron cooling due to SIN tunnel junctions to be the dominant process.

The CEB concept is based on the direct electron cooling of the absorber that serves as a negative electrothermal feedback for the incoming signal. The electromagnetic signal is first detected by the antenna. It then goes through the superconductor-insulator-normal metal (SIN) tunnel junctions to the normal metal absorber. The energy is then absorbed by the electrons in the absorber. One electron has obtained an energy equal to the energy of one photon. The first step in the relaxation process is due to electron-electron interaction. At this point, there is a number of hot electrons with high energies.

The next step in the relaxation of energy is brought about by two processes. The first process is due to electron-phonon interaction in the absorber. The second is due to electron cooling by the SIN tunnel junctions. The ideal case would be to transfer all the high energy electrons through the tunnel junctions, which is seen as a current response.

To make this response as close to ideal as possible, we employed proximity traps to enhance the electron cooling of the absorber, which serves as a negative electrothermal feedback. This type of feedback keeps the electron temperature below the phonon temperature. This improves the detector responsivity and sensitivity. The feedback also increases the dynamic range of the device.

II. Theory of the Cold-Electron Bolometer

The non-equilibrium theory of the hot-electron bolometer (HEB) is explained in detail by Golubev and Kuzmin [5]. In this HEB, the absorber is capacitively-coupled to the antennae through SIN tunnel junctions. As described previously, the electron temperature, T_e in the CEB is kept well below phonon temperature, T_{ph}. This is achieved by improving the geometry of the superconducting electrodes such that there is more volume for tunneled quasiparticles to diffuse into, or by adding normal metal traps adjacent to the superconducting electrodes [6], [7]. The only effect of this is to increase the cooling power of the SIN tunnel junction. This cooling power is well described in equation (2) below and no change in any of the expressions below is necessary to account for conceptual differences between the HEB and the CEB.

As previously stated, the electron temperature of the absorber is related to the power of the incoming radiation, which we are interested in measuring. In order to determine the electron temperature of the normal metal absorber, one has to take into account all the contributions to the heat load to the absorber. The dominant power contribution at a given bias voltage at a certain temperature will determine the electron temperature. This can be attained by solving the heat balance equation, as shown below.

$$c_v \nu \frac{dT}{dt} + \Sigma \nu \left(T_e^5 - T_{ph}^5\right) + P(V, T_e, T_S) = P_0 + \frac{V^2}{R_s} + \delta P(t) \qquad (1)$$

where $c_V = \gamma T_e$ is the specific heat of the normal metal, ν is its volume, $\Sigma\nu(T_e^5 - T_{ph}^5)$ is the heat flow from the electron to the phonon sub-system in the normal metal, Σ is the electron-phonon coupling constant dependent on the material used, ν is the volume of the absorber, V^2/R_S is the heat load due to the subgap leakage resistance, R_S, P_0 is the background optical power load of the bolometer, $\delta P(t)$ is the incoming rf power. The cooling power, $P(V,T_e,T_S)$, of the SIN tunnel junction is given by:

$$P(V, T_e, T_S) = \int dEE\left[\Gamma_{N\to S}(E) - \Gamma_{S\to N}(E)\right] \qquad (2)$$

In the calculations, the temperature of the superconductor, T_S is assumed to be equal to the phonon temperature, T_{ph}. In general, this is not the case and heating of the superconducting electrodes should be considered. However, we are interested in the region below the superconducting gap where the absorber is cooled due to the dominant cooling power of the tunnel junction.

A bolometer is characterized by its responsivity and sensitivity and its time constant. In the current-biased mode, the responsivity, S_V, is described by the voltage response to an incoming power

$$S_V(\omega, I) = \frac{\delta V_\omega}{\delta P_\omega} = \frac{-\dfrac{\partial I/\partial T}{\partial I/\partial V}}{-i\omega c_V \nu + 5\Sigma \nu T_e^4 + \dfrac{\partial P}{\partial T} - \dfrac{\partial I/\partial T}{\partial I/\partial V}\dfrac{\partial P}{\partial V}} \qquad (3)$$

The noise is characterized by the Noise Equivalent Power (NEP), which is the net effect of all the sources referred to the input of the bolometer. The total NEP is the sum of three components given by

$$\mathrm{NEP}_{\mathrm{total}}^2 = \frac{\left\langle \delta V_\omega^2 \right\rangle_{\mathrm{amp}}}{S_V^2(0, I)} + 10 k_B \Sigma V\left(T_e^6 + T_{ph}^6\right) + \mathrm{NEP}_{\mathrm{NIS}}^2 . \qquad (4)$$

The first term on the right hand side is the NEP due to the amplifier given by the voltage noise of the amplifier divided by the voltage response of the bolometer to applied power. The second term is the NEP associated with the heat flow between electrons and phonons. The last term is the NEP associated with NIS tunnel junction. Theory predicts that the CEB should be able to show a sensitivity of 10^{-19} W/Hz$^{1/2}$. This paper demonstrates a sensitivity of better than 10^{-18} W/Hz$^{1/2}$ at 100 mK in the current-bias mode.

The CEB for dc characterization is composed of four superconductor-insulator-normal metal (SIN) tunnel junctions. The outer SIN junctions serves as a capacitive coupling of the absorber to the antenna, as thermal isolation and as electron coolers of the absorber. All these three functions work for the improvement of the responsivity and the sensitivity of the bolometer. Chouvaev, et. al. [8] reported that the improvement is due to the isolation of the device from the external interferences picked-up by the lead wires. Jochum, et. al. [9] demonstrates the significance of the temperature of the normal metal to the increased sensitivity of detectors which utilize SIN tunnel junctions. The inner SIN junctions serve to measure the temperature of the normal metal. For this purpose, these junctions should have minimal influence on the device. To do this, the inner tunnel junctions were designed to have smaller area in comparison to the outer tunnel junctions.

As was mentioned, the detector sensitivity is improved by electron cooling of the absorber. The addition of normal metal traps adjacent to the outer SIN tunnel junctions greatly enhances the electron cooling. In our previous work [6], [7], we demonstrated a decrease in electron temperature by almost 200 mK with the use of the normal metal traps. With all these

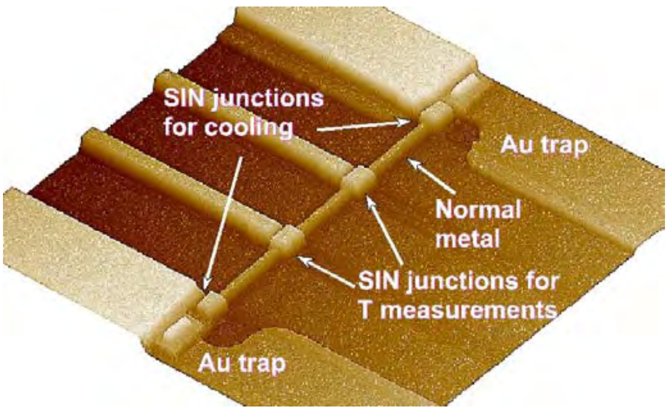

Fig. 2. Atomic force microscope image of a typical cold-electron bolometer. The outer SIN tunnel junctions cools the electrons in the normal metal. This electron cooling is enhanced by the Au traps in proximity to the cooling junctions. The inner SIN tunnel junctions acts as a thermometer to measure electron temperature in the absorber.

TABLE I
LIST OF EXPERIMENTAL PARAMETERS

	Area (μm2)	Normal Resistance (kΩ)	Zero-bias Resistance (MΩ)
Outer SIN tunnel junctions	0.45	4.3	8.4
Inner SIN tunnel junctions	0.06	14.5	21.2
Normal metal absorber	0.11 μm^3 [a]	0.063	-

Measured parameters at 20 mK. The normal resistance corresponds to the asymptotic resistance for large bias currents.

[a]The volume of the absorber is the important parameter as it is directly coupled to the absorbed power and therefore to the sensitivity of the device.

things in consideration, we have fabricated our device as follows.

III. Fabrication of the Device

The CEB is fabricated by e-beam lithography using two-layer resist technology, and two-angle evaporation. 0.2 μm PMMA on top of 0.8 μm Copolymer were exposed to 80 pA of beam current with a dose of 315 $\mu C/cm^2$. PMMA was developed in Toluene:IPA=1:3 and Copolymer in Ethoxylacetate:Ethanol=1:5 to create the masks for the device pattern. The normal metal traps and the bolometer device were made in two separate vacuum cycles. In the first vacuum cycle, 10 nm of chromium, followed by 30 nm of gold, and finally 10 nm of palladium were thermally evaporated to make 50 nm of normal metal trap. Cr was used for better adhesion of Au to the SiO_2 substrate. Pd was used as a buffer layer between Au and Al when they are in contact with each other. In time, Au reacts with Al forming an alloy that increase the contact resistance, which is naturally undesirable.

In the second vacuum cycle, the aluminum electrode was thermally evaporated at an angle of 55º relative to the surface normal upto a thickness of about 60 nm. The tunnel barrier was formed by oxidizing the electrode for 2 minutes at a pressure of 5×10^{-2} mbar. The normal metal absorber was created by evaporating 30 nm of chromium and then 30 nm of copper at an angle of 0º. Cr was used to improve the impedance matching of the antennae to the normal metal and also for better adhesion of Cu to the substrate. The measured resistance of the absorber was about 60 Ω. Table 1 lists down the pertinent experimental parameters of the CEB. Fig. 2 shows a typical schematic of the CEB using a scanning probe microscope.

The sample was measured in an Oxford dilution refrigerator. Measurements were performed in the current-biased mode. The current source consisted of a symmetric voltage source in series with bias resistors ranging from 200 kΩ to 20 GΩ. This provides us the possibility to measure large voltage ranges to measure the asymptotic resistances of the junctions, and also their subgap and zero-bias resistances. The high-ohmic bias resistances also provide some amount of protection from external interference.

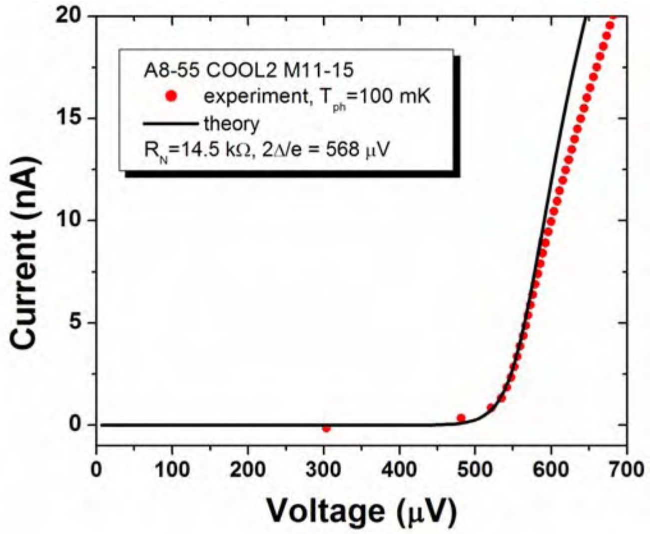

Fig. 3. Current-voltage characteristic of the tunnel junction used for response measurements (the inner pair) at T_{ph}=100 mK (circles). The measured normal state resistance was 14.5 kΩ and the subgap resistance was 21.2 MΩ. The superconducting gap, 2Δ=568 μeV, was estimated by fitting the theoretical curve (solid line) with the experimental curve.

IV. Results and Analysis

A. I-V Characteristics

Fig. 3 shows the current-voltage characteristic of the inner tunnel junctions, which was used as the response junctions. The superconducting gap voltage of 568 μeV for the aluminum electrode was estimated by fitting the theoretical estimate with the experimental data. The solid line shows the theoretical fit. It is in very good agreement in the region of the gap. As the voltage increases from the gap voltage, the discrepancy between the theory and experiment increases. Moving further away from the gap (not shown), the discrepancy then decreases, and the experimental curve follows the asymptotic line corresponding to the normal state resistance of the tunnel junction pair. We believe that the discrepancy is due to nonuniformity of the gap in the tunnel junction.

B. Bolometer Responsivity, dV/dP

The basic idea in measuring bolometer responsivity in the current-biased mode is the determination of the voltage response corresponding to an input power. We have used both dc input power and modulated input power with frequencies from 35 Hz to 2 kHz, and measured voltage response in both cases.

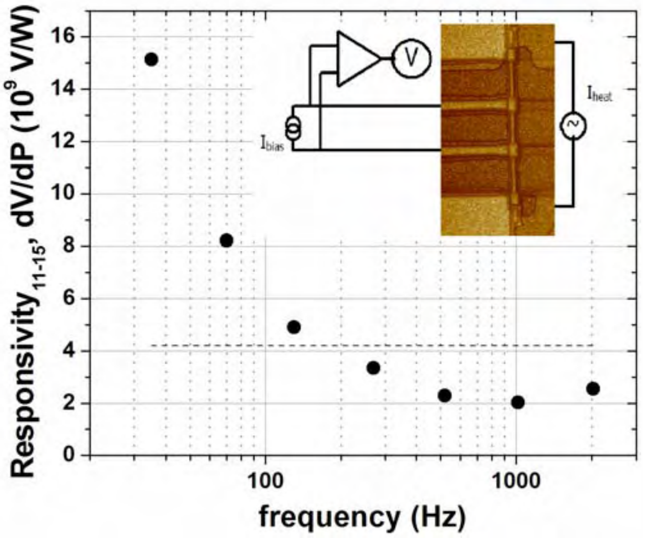

Fig. 4. Measured responsivity of the inner tunnel junctions at T_{ph}=100 mK (circles) for modulation frequencies from 35 Hz to 2.02 kHz. Using the experimental parameters, the theoretical curve (dashed line) predicted a responsivity of 4.2x10^9 V/W. (Inset) A view of the measurement scheme for responsivity.

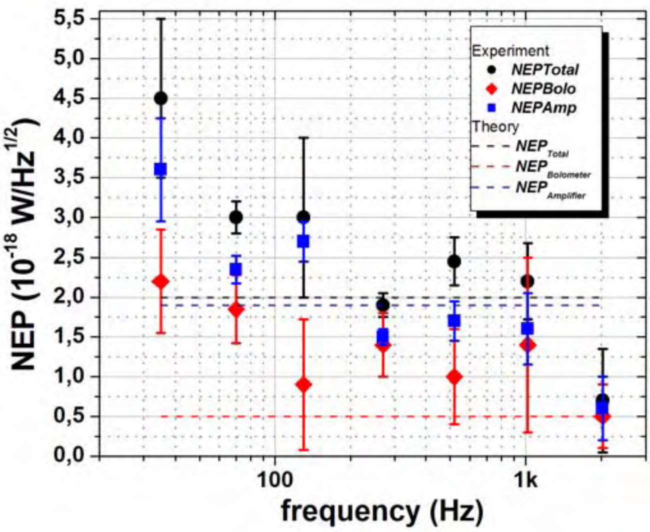

Fig. 6. Measured noise equivalent power (*NEP*) of the inner tunnel junctions for modulation frequencies from 35 Hz to 2.02 kHz. The dashed lines show the theoretical estimations using the experimental parameters. The bolometer *NEP* is clearly better than 10^{-19} W/Hz$^{1/2}$ for modulation frequencies above 100 Hz. Theory predicts 5x10^{-19} W/Hz$^{1/2}$ for the given experimental parameters.

To measure the response of the inner junctions, we applied the input power to the outer junctions. The technique with dc input power requires sweeping an external current bias to the outer junctions. Using its I-V characteristic, we can determine how much power we are applying to the absorber. The corresponding voltage response is measured for different bias currents of the inner junctions. Using the I-V characteristic of the inner junctions, the maximum responsivity, *dV/dP* can then be plotted as a function of the bias voltage.

In the modulation technique, a modulated bias current is applied to the outer tunnel junctions. Using its I-V characteristic, the magnitude of the input power can be obtained. We have then measured the voltage response using the SR830 lock-in amplifier by sweeping the bias to the inner tunnel junctions. Figure 4 shows the result of our measurement of responsivity for different frequencies using the modulated heating power. The highest value of the responsivity obtained at 35 Hz was measured to be 1.5x10^{10} V/W. The attenuation of the filter lines in the dilution refrigerator is the most probable reason for the observed dependence of responsivity on frequency. The dashed line shows the responsivity computed from theory using the experimental parameters. Theory gives the value for maximum responsivity of 4.2x10^9 V/W.

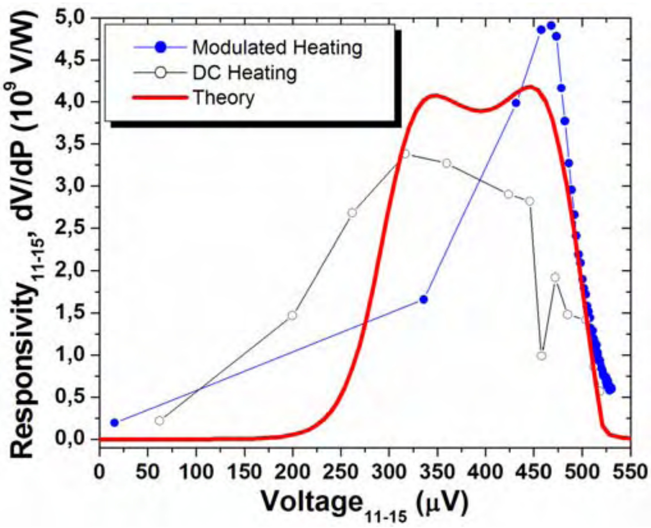

Fig. 5. Comparison between the two techniques of measuring the bolometer responsivity and the theoretical estimation.Very good agreement between experiment and theory can be seen in the region near and below the superconducting gap voltage.

Fig. 5 shows comparison between responsivities measured using dc heating power, modulated heating power of 0.2 fW for f = 120 Hz and the theoretical result from the experimental parameters. In the region below the gap where it is expected to have good electron cooling, both experimental curves agree well with the theory.

C. Bolometer NEP

The next step in the characterization was to measure the *NEP* of the bolometer. It can be only be measured indirectly by subtracting the amplifier NEP from the total NEP, i.e.

$$NEP_{total}^2 = NEP_{bolometer}^2 + NEP_{amplifier}^2 \qquad (5)$$

The total *NEP* and the amplifier *NEP* is obtained by the dividing the responsivity by the total noise and the amplifier noise, respectively, as described in (4). Fig. 7 shows the measured total *NEP*, amplifier *NEP*, and bolometer *NEP* as a function of frequency of modulated heating. We have observed bolometer *NEP* to be better than 10^{-18} W/Hz$^{1/2}$ for modulation frequencies greater than 100 Hz. Theoretical estimations give NEP_{total} = 2x10^{-18} W/Hz$^{1/2}$, $NEP_{amplifier}$ = 1.8x10^{-18} W/Hz$^{1/2}$, and $NEP_{bolometer}$ = 5x10^{-19} W/Hz$^{1/2}$ (shown in dashed lines).

Fig. 7 shows the *NEP* as a function of voltage at f = 1.02 kHz in comparison to theory. Below the gap region, we see a good qualitative agreement between experiment and theory to within the accuracy of measurement.

The main limitation to our measurement of bolometer NEP is the large noise contribution of the amplifier. This can be improved by using an amplifier with lower voltage noise, or a cold amplifier to reduce its thermal noise. Another method would be to improve the noise temperature by operating the amplifier with higher source impedance. The source impedance for a typical amplifier such as OPA111 is in the order of MΩ. However, the resistance of our device is in the order of kΩ at the optimal bias. To achieve the high source impedance, the superconducting CEB (SCEB) is proposed [10]. In the SCEB, the operating point would be in the region between the difference and the sum gap. In that region, the impedance is in the order of MΩ, which is desirable for the operation of a room temperature amplifier with lower noise temperature. In addition, analysis of the CEB made by Golubev and Kuzmin [5] show that the voltage-biased regime is optimal for better responsivity and sensitivity.

D. Estimation of time constants

To fully characterize the bolometer, we estimated the time constants of the electron-phonon interaction and the extraction of normal metal electrons due to cooling by the SIN tunnel junctions using the experimental parameters. The time constant is given by

$$\tau = \frac{\gamma T_e v}{\partial P_{total} / \partial T} \qquad (6)$$

where

$$\partial P_{total} / \partial T = \partial P_{e-ph} / \partial T + \partial P_{cool} / \partial T \qquad (7)$$

For the normal metal absorber, we used γ=9.77 J/μm^{3}K^2 for

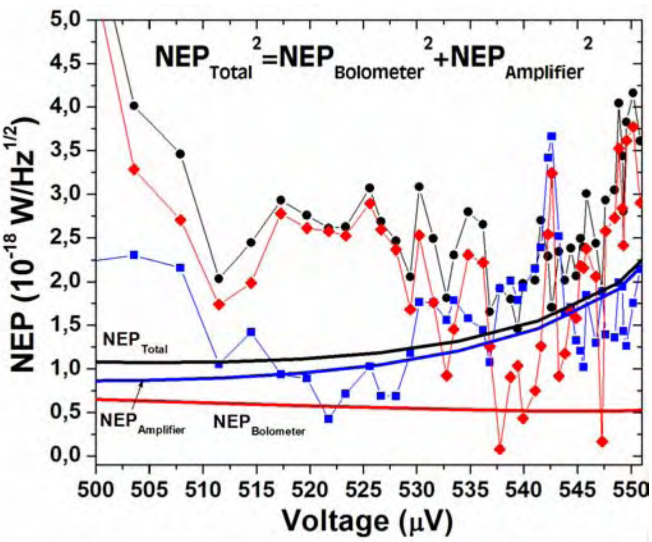

Fig. 7. The measured noise equivalent power (*NEP*) near and below the superconducting gap voltage for f = 1.02 kHz in comparison to theoretical prediction. In the region near the gap, there is a good qualitative agreement between experiment and theory.

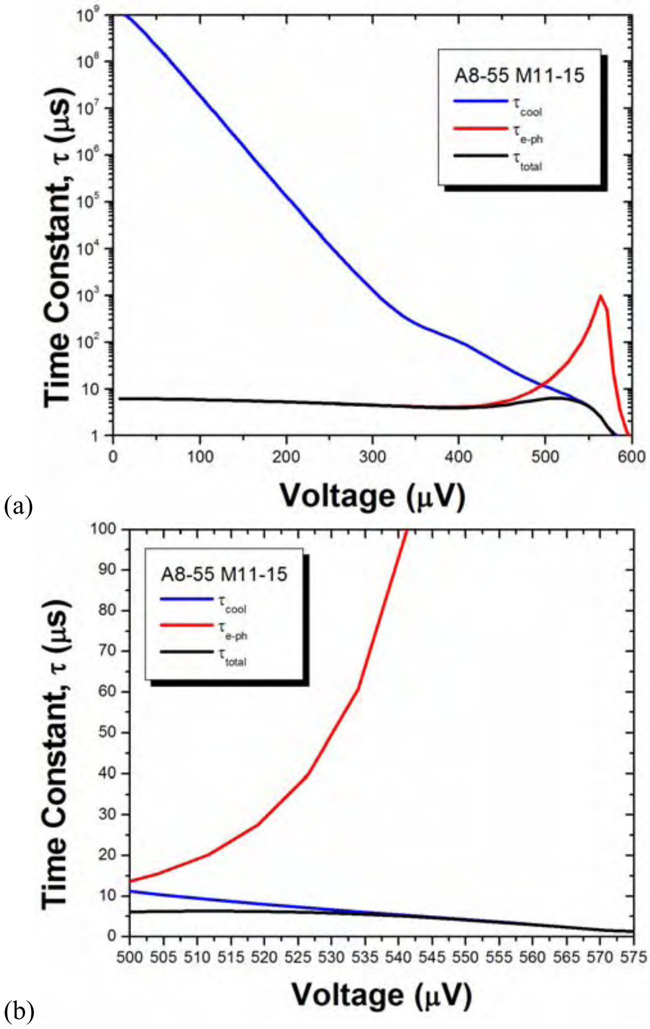

Fig. 8. Estimation of time constants using the experimental parameters. (a) In the subgap region, the dominant process is due to the electron-phonon coupling. (b) In the region near and below the gap, the dominant process is the electron cooling due to the SIN tunnel junctions.

copper. Fig. 8a shows our estimation for all relevant voltage ranges. In the subgap region where the dynamic resistance is high, the dominant process is clearly the interaction due to electron-phonon coupling. As the bias approaches the superconducting gap, the electron cooling begins to take over. In region just below the gap, the dominant process is the cooling of the SIN tunnel junctions. This is more clearly depicted in fig. 8b.

V. CONCLUSIONS

We have fabricated and characterized the cold-electron bolometer (CEB). We have measured the responsivity by applying an input power from a modulated heating current for frequencies from 35 Hz to 2.02 kHz. The best value of the responsivity obtained was 15x10^9 V/W for f = 35 Hz. We have also measured the noise equivalent power of the bolometer. For modulation frequencies greater than 100 Hz, the measured *NEP* is better than 10^{-18} W/Hz$^{1/2}$. Theory gives good agreement with the experimental results in the region near and below the superconducting gap voltage. In this region, the estimated time constant is mainly due to the strong electron cooling of the normal metal absorber by the SIN tunneling junction.

ACKNOWLEDGMENT

We would like to thank Dmitry Golubev for extensive and enlightening discussions on the theoretical part of this work.

REFERENCES

[1] D. Leisawitz et al., “Scientific motivation and technology requirements for the SPIRIT and SPECS far-infrared/submillimeter space interferometers”, SPIE 2000.

[2] K. Irwin, “An application of electrothermal feedback for high-resolution cryogenic particle detection,” *Appl. Phys. Lett.*, vol. 66, no. 15, pp. 1998-2000, Apr. 1995.

[3] A. Lee, P. Richards, S. W. Nam, B. Cabrera, K. D. Irwin, “A superconducting bolometer with strong electrothermal feedback,” *Appl. Phys. Lett*, vol. 69, no. 12, pp. 1801-1803, Sep. 1996.

[4] L. Kuzmin, “Ultimate cold-electron bolometer with strong electrothermal feedback,” *Proceedings of SPIE -- Millimeter and Submillimeter Detectors for Astronomy II*, vol. 5498, pp. 349-361, Oct. 2004.

[5] D. Golubev and L. Kuzmin, “Non-equilibrium theory of a hot-electron bolometer with normal metal-insulator-superconductor tunnel junction,” *J. of Appl. Phys*, vol. 89, no. 11, pp. 6464-6472, Jun. 2001.

[6] I. J. Agulo, L. Kuzmin, M. Fominsky, and M. Tarasov, “Effective electron microrefrigeration by superconductor-insulator-normal metal tunnel junctions with advanced geometry of electrodes and with normal metal traps,” *Nanotechnology*, vol. 15, no. 4, pp. S224-S228, Apr. 2004.

[7] L. Kuzmin, I. J. Agulo, M. Fominsky, A. Savin, and M. Tarasov, “Optimization of electron cooling by SIN tunnel junctions,” *Supercond. Sci. Technol.*, vol. 17, pp. S400-S405, May 2004.

[8] D. Chouvaev, L. Kuzmin, and M. Tarasov, “Normal-metal hot-electron microbolometer with on-chip protection by tunnel junctions,” *Supercond. Sci. Technol.*, vol. 12, no. 11, pp. 985-999, Nov. 1999.

[9] J. Jochum, C. Mears, S. Golwala, B. Sadoulet, J. P. Castle, M. F. Cunningham, O. B. Drury, M. Frank, S. E. Labov, F. P. Lipschultz, H. Netel, and B. Neuhauser, “Modeling the power flow in normal conductor-insulator-superconductor junctions,” *J. of Appl. Phys.*, vol. 83, no. 6, pp. 3217-3224, Mar. 1998.

[10] L. Kuzmin, “Superconducting Cold-electron bolometer with proximity traps,” *Micr. Eng.*, vol. 69, no. 2-4, pp. 309-316, Sep. 2003.